HHS Public Access

Author manuscript

Ann Biomed Eng. Author manuscript; available in PMC 2017 April 01.

Published in final edited form as:

Ann Biomed Eng. 2016 April ; 44(4): 954–967. doi:10.1007/s10439-015-1398-0.

Regurgitation hemodynamics alone cause mitral valve remodeling characteristic of clinical disease states in vitro

Patrick S. Connell, BS[1], **Anam F. Azimuddin, BS**[1], **Seulgi E. Kim**[1], **Fernando Ramirez**[1], **Matthew S. Jackson, MS**[2], **Stephen H. Little, MD**[2], and **K. Jane Grande-Allen, PhD**[1]

[1]Rice University, Department of Bioengineering, Houston, TX

[2]Houston Methodist Hospital, Department of Cardiology, Houston, TX

Abstract

Mitral valve regurgitation is a challenging clinical condition that is frequent, highly varied, and poorly understood. While the causes of mitral regurgitation are multifactorial, how the hemodynamics of regurgitation impact valve tissue remodeling is an understudied phenomenon. We employed a pseudo-physiological flow loop capable of long-term organ culture to investigate the early progression of remodeling in living mitral valves placed in conditions resembling mitral valve prolapse (MVP) and functional mitral regurgitation (FMR). Valve geometry was altered to mimic the hemodynamics of controls (no changes from native geometry), MVP (5mm displacement of papillary muscles towards the annulus), and FMR (5mm apical, 5mm lateral papillary muscle displacement, 65% larger annular area). Flow measurements ensured moderate regurgitant fraction for regurgitation groups. After 1-week culture, valve tissues underwent mechanical and compositional analysis. MVP conditioned tissues were less stiff, weaker, and had elevated collagen III and glycosaminoglycans. FMR conditioned tissues were stiffer, more brittle, less extensible, and had more collagen synthesis, remodeling, and crosslinking related enzymes and proteoglycans, including decorin, matrix metalloproteinase-1, and lysyl oxidase. These models replicate clinical findings of MVP (myxomatous remodeling) and FMR (fibrotic remodeling), indicating that valve cells remodel extracellular matrix in response to altered mechanical homeostasis resulting from disease hemodynamics.

Keywords

Mitral valve regurgitation; Mitral valve prolapse; Functional mitral regurgitation; Organ culture; Myxomatous remodeling

Address for Correspondence: K. Jane Grande-Allen, Rice University MS142, 6100 Main St., Houston, TX 77005, Telephone Number: 713-348-3704, Fax Number: 713-348-5877, grande@rice.edu.

Conflicts of Interest

Dr. Stephen H. Little has received research funds from St. Jude Medical, Medtronic Inc, Abbott Vascular Structural Heart. Dr. Jane Grande-Allen has served as a consultant for Edwards Lifesciences. Other authors have no disclosures.

Introduction

Mitral valve regurgitation is an insidious, frequent, and heterogeneous condition with a lack of fundamental knowledge about how this disease starts, progresses, or could be reversed or prevented. Despite a wide variety of clinical presentations, all mitral regurgitation is accompanied by a distortion of valve geometry, resulting in valves experiencing an altered hemodynamic profile. These alterations change the mechanical forces the valves experience throughout the cardiac cycle.[25,29,38] It has been previously shown that valve interstitial cells are sensitive to changing mechanical environments, and that changes in strain can alter the types of extracellular matrix proteins that valve interstitial cells produce and degrade.[33,34] In light of these findings, it is clear that the impact of altered regurgitation hemodynamics on the remodeling of valve tissues throughout the progression of mitral regurgitation is an understudied phenomenon.

The two main types of mitral regurgitation result in vastly different hemodynamic profiles, and the valves in each experience very different mechanical forces. Organic mitral regurgitation typically takes the form of mitral valve prolapse (MVP). MVP is associated with slack tissues, resulting in decreased tension experienced by valve components.[24,27] MVP is also associated with the mechanical weakening of valve tissues, including leaflets and chordae tendineae, as well as an accumulation of glycosaminoglycans (GAGs) and proteoglycans within tissues, a process known as myxomatous remodeling.[22] MVP is multifactorial, with a variety of molecular and genetic factors altered across different patient populations with the disease.[14] Despite new insight into potential genetic or molecular mechanisms of myxomatous degeneration, there remain gaps in our knowledge of how MVP initiates and progresses.[14]

The second type of regurgitation, functional mitral regurgitation (FMR), develops as a result of the distortion of the valve annulus and papillary muscle geometry that occurs in regional or global left ventricular systolic dysfunction.[44] The altered geometry creates higher tension forces throughout the leaflets and chordae of the valve, resulting in leaflet tethering.[25,29] Tethering prevents appropriate valve coaptation during systole, resulting in backflow. Overall, FMR is associated with stiffer, more fibrotic tissues.[19,20]

These two disease processes represent not only the different etiologies of mitral regurgitation, but also the extremes of functional disturbance and altered geometry. Despite the detailed findings of studies into the mechanical and compositional properties of both end-stage MVP and FMR tissues,[19–22] how the altered mechanical environment of regurgitation directly impacts these properties remains poorly understood. By understanding the impact of the extremes of high and low tension, we gain an appreciation for the valve interstitial cell response to altered mechanics and the impact mechanics has on the progression of mitral regurgitation.

Our group has designed a pseudo-physiologic flow loop system, the Rice University Flow Loop System (RUFLS), capable of long-term *in vitro* culture of living mitral valves.[18] Here we document the ability to recreate the hemodynamic environment of both MVP and FMR *in vitro* using RUFLS. We then explore how the resulting altered mechanics affect valve

interstitial cell remodeling of the underlying extracellular matrix and posit that the differences observed in the tissue characteristics of these two disease conditions are influenced by the natural responses of cells to altered tension.

Materials and Methods

Organ Culture System

The design and operation of the core components of RUFLS have been described previously.[17,18] In brief, adolescent (6 to 9 month) porcine mitral valves obtained from a local abattoir (Fisher's Ham and Meats, Spring, TX) are harvested intact and installed into a mitral valve holder. This mitral holder is then placed into a mock left ventricular chamber. The left ventricular chamber is comprised of a culture medium compartment and an air compartment separated by a silicone membrane. LabView software (National Instruments, Austin, TX) powers a proportional pressure regulator (Numatics, Novi, MI) that creates a high-pressure systolic waveform that forces media through a mechanical aortic valve and into the flow loop. Other loop components include a compliance chamber, which dampens the systolic pressure wave, and a reservoir chamber, which holds media until it flows by gravity back through the mitral valve for a low-pressure filling phase and has an attached air filter for air exchange within the system. The system creates a complete mock cardiac cycle with physiological waveforms and pressures, with a flow rate of 3 liters per minute. For this study, approximately 1.2 L of M199 culture medium (Sigma-Aldrich, St Louis, MO) supplemented with 10% bovine growth serum (ThermoHyclone, Logan, UT) and 2% anti-microbial solution (Mediatech, Manassas, VA) was pumped through each loop at a rate of 60 beats per minute and a systolic pressure of 125mmHg. The system was placed in a standard cell culture incubator at 37°C and 5% CO_2. A schematic of the system is shown in Figure 1.

Imaging Flow Loop

A second, non-sterile, imaging flow loop, described in detail previously,[35,36] was used to visualize valve movement and hemodynamics of control and disease models cultured in RUFLS. This system was augmented to allow for installation of intact mitral valves within its mock left ventricular chamber using the same attachment mechanisms as RUFLS. Using this flow loop, we recreated flow conditions of moderate mitral regurgitation in order to confirm the functional abnormalities of each mitral regurgitation condition. Incorporated into this system were imaging windows capable of visualization and ultrasound, including color Doppler echocardiography (2 to 4 MHz transducer, Sonos 7500, Philips Medical Systems, Bothell, Washington), at standard anatomic positions and distance.

Creation of Experimental Culture Conditions

Improvements to the organ culture system since it was first published,[17] allow for precise control of the position of the papillary muscles independently along both the apical-basal and medial-lateral axes (Supplemental Figure 1). Prior to harvest, papillary muscle position was determined by measuring the distance to the corresponding valve commissure in both the apical-basal and the medial-lateral axes. For the purposes of papillary muscle positioning it was assumed the papillary muscles were positioned directly below the commissures along the anterior-posterior axis. The annular size of the mitral valve was then determined using a

Duran AnCore annuloplasty ring sizing kit (Medtronic, Minneapolis, MN). These measurements were considered the neutral position of the valve apparatus and were replicated for control models.

To create the slack chordae and low tension associated with MVP, harvested valves were first placed in the neutral position and then both papillary muscles were displaced 5 mm basally, towards the annulus.

To create the high-tension tissues associated with FMR, harvested valves were first sewn onto annular rings approximately 65% larger by area than control annuli. This greater area included a 10% greater commissure-to-commissure dimension and a 50% greater anterior-posterior annular measurement. These altered dimensions were based on a variety of clinical findings comparing patients with FMR to controls[7,20,39] and values used to create *in vitro* FMR.[11,25,37] The harvested valves were then placed in the neutral position and papillary muscles were displaced 5 mm apically, away from the valve annulus, and 5 mm laterally, creating the high-tension tethering of FMR. These displacements have been previously shown to elevate tension on anterior strut, posterior basal, and commissural chordae, thereby increasing leaflet tenting and regurgitation.[25,29] Alterations in valve geometry for both MVP and FMR models can be seen in Figure 2.

All models were cultured in RUFLS for one week and monitored for regurgitant flow and cardiac output using an ultrasonic meter (Transonic Systems, Ithaca, NY). After culture, select valves were imaged using both video and color Doppler echocardiography in our imaging flow loop to characterize regurgitant flow of different models. All valves were then sectioned with leaflets divided into either radial or circumferential direction sections as seen in Figure 3. Radial dissection resulted in anterior radial and posterior radial leaflet segments and anterior basal, anterior marginal, posterior basal, and posterior marginal chordae for use in mechanical and histological studies. Circumferential sections resulted in anterior clear zone, anterior rough zone, and posterior circumferential sections along with the chordal sections for use in mechanical and biochemical testing.

Validation of Viability of Control Condition Tissues

To verify that improvements made to the RUFLS system did not affect tissue viability, a series of assays were performed as described previously.[18] Fresh porcine mitral valves were obtained and sections were compared to control conditioned tissues cultured for 1 week to ensure viability of tissues within the system (n = 6). DNA content was assessed using fluorescent Picogreen dye (Invitrogen, Grand Island, NY) and valve layer structure was analyzed by Movat pentachrome stain. In addition, to ensure the viability of cells from cultured valves, cells were isolated from control condition valve leaflets and cultured on tissue culture plastic for 2 weeks as previously described.[45]

Histological Staining and Immunohistochemistry

Radial sections reserved for histology or immunohistochemistry were formalin-fixed, paraffin embedded, and sectioned into 5 μm thick sections. Tissue sections from each condition were then stained according to previously described methods using a Herovici stain, used to differentiate between young collagen, stained blue, and mature collagen,

stained red.[26] Picrosirius red staining was used to assess collagen alignment according to the color observed under polarized light with more aligned collagen producing longer wavelengths (i.e. red) of birefringence.[13,30]

Immunohistochemistry analysis was performed using techniques previously described.[46] This analysis allowed for localization of several markers of tissue phenotype and collagen remodeling, including collagen III (ab7778; Abcam, Cambridge, England), matrix metalloproteinase-1 (MMP-1; ADI-905-472-1, Enzo Life Sciences, Farmingdale, NY), decorin (LF # 136, Gift from Dr. Larry Fisher, NIH),[15] lysyl oxidase (LOX; IMG-6442A, Imgenex, San Diego, CA), and prolyl-4-hydroxylase (P4H; bs-5090R, Bioss, Woburn, MA). A biotinylated secondary antibody (Jackson Immunoresearch, West Grove, PA) was added to all samples to allow for visualization using a 3,3′-Diaminobenzidine chromagen reaction (Vector Laboratories, Burlingame, CA). Negative controls for each secondary antibody were performed for each sample with no primary antibody.

For both histology stains and IHC, the anterior leaflet clear zone, anterior leaflet rough zone, and posterior mid-leaflet regions were imaged using a Leica DMLS upright light microscope (Buffalo Grove, IL). Herovici staining was imaged using white light, while picrosirius red stain images were conducted under both white light and polarized light in order to capture the birefringence of the constitutive collagen fibers.[13,30] For Herovici and picrosirius red birefringence analysis, Image J software (NIH, Bethesda, MD) was used to first split images into their hue, saturation, and brightness components and then quantify the amount of red hue present as a percentage of total tissue area as described previously.[43] IHC analysis was performed as previously described using Image J software to determine the percent of tissue area that stained positive for the antigen of interest compared to matched negative control (n = 6 to 8 for all staining).[2]

Materials Testing

Mechanical analysis was performed as described previously.[18] Anterior clear zone, anterior rough zone, anterior radial, posterior circumferential, and posterior radial leaflet segments (each n = 6 to 8) and anterior basal, anterior marginal, posterior basal, and posterior marginal chordae (each n = 14 to 16, 2 of each type tested per valve) were tested with a pre-determined uniaxial tensile testing protocol using an EnduraTEC ELF 3220 (Bose, Eden Prairie, MN).

In brief, thickness, width, and gauge length of the tissue segments were measured prior to testing. Testing was conducted in 37°C phosphate buffer saline. Tissue was preconditioned using ten load-unload triangle waves. A simple ramp load was then applied and held for 60 seconds to measure stress relaxation. This evaluation was followed by a ramp unload, 10 second rest period, five preconditioning cycles and a simple load-unload triangle wave to observe tissue hysteresis. The tissue segment was then stretched to failure. Any sections that failed prior to completion of the entire protocol were not included in the analysis.

Mechanical testing data was then converted from load and displacement to stress-strain curves for analysis conducted using MATLAB software (MathWorks, Natick, MA). Gauge length for each test was determined according to protocols developed from previously

described methods.[8] Stress relaxation data was fit to a bi-phasic decay model and the fast and slow time constants were calculated. Hysteresis percentage was calculated by dividing the area between the loading and unloading curve by the total area under the loading curve. Elastic modulus was calculated from the slope of the second linear region of the bilinear stress-strain curve, extensibility was calculated as the x-intercept of the line defined by the elastic modulus, and the ultimate stress and strain were defined as the stress and strain values at the maximum stress obtained throughout failure tensile testing.

Biochemical Analysis

Biochemical analysis was conducted as previously described.[18] Anterior clear zone, anterior rough zone, and posterior leaflet sections (n = 7 to 8) were weighed before and after lyophilization to determine hydration of tissues. After digestion in pepsin (Sigma-Aldrich, St. Louis, MO), samples were tested for collagen content using the Sircol Assay (Biocolor, Carrickfergus, United Kingdom). After digestion in both pepsin and Proteinase K (Calbiochem, Darmstadt, Germany), samples were tested for GAG content using the Blyscan Assay (Biocolor, Carrickfergus, United Kingdom). Colorimetric data was analyzed using a Spectramax M2 (Molecular Devices, Sunnyvale, CA) and compared to standard curves prepared using known quantities of rat-tail collagen or glucuronic acid for the Sircol or Blysacn assay, respectively. All values were normalized to dry weight of the tissue sample.

Statistical Analysis

Statistical analysis was performed using R Studio software (Version 0.98.953). Data are expressed as mean ± standard error or as percent difference of the means. Graphs are expressed as boxplots with outliers being defined by the 1.5 interquartile range rule. Unless otherwise stated, two-way ANOVA with post hoc Tukey Honestly Significant Difference test was performed to determine differences across condition groups (control vs. MVP and control vs. FMR) and tissue sections (i.e. anterior rough vs. anterior clear). When the patterns of results were inconsistent across tissue sections, individual one-way ANOVA with post hoc Tukey test was performed across condition groups to determine differences. Power analysis was performed to ensure appropriate sample size for all groups ($1-\beta = 0.8$). Results were considered significant at $p < 0.05$.

Results

Validation of Control Condition Valve Viability

No significant difference was found in valve thickness or DNA content comparing control condition to fresh valve tissues. In addition, observation of the layered structure of valve tissues using Movat pentachrome staining showed no phenotypic difference between valve tissues from the control condition or fresh sources. Cells isolated from control condition tissues were successfully cultured for two weeks on tissue culture plastic and demonstrated growth rates consistent with cells obtained from fresh tissues (data not shown).

Hemodynamic Validation of Disease-Mimicking Conditions

Flow measurements obtained at the end of one-week culture showed moderate regurgitation in MVP (regurgitant fraction 35 ± 4%) and FMR (regurgitant fraction 20 ± 2%) conditions. In contrast, low regurgitation was observed and maintained in controls (regurgitant fraction 11 ± 1%). Both conditions also experienced a significant increase from the degree of regurgitation at the initial setup to the final amount of regurgitation across the one-week culture (MVP: +13 ± 4%, $p < 0.05$; FMR: +8± 1%, $p < 0.001$, Student's t test).

In addition, color Doppler echocardiography performed using the imaging flow loop after one-week culture confirmed that MVP condition valves displayed the characteristic eccentric regurgitant jet of prolapse and that FMR condition valves displayed the characteristic central jet of FMR (Figure 4 and Supplemental videos 1–3). Standard clinical echocardiogram measurements were also performed on the imaged valves. Regurgitant volumes obtained using a flow meter, vena contracta orifice area, and proximal isovelocity surface area (PISA) orifice area and regurgitant volume confirmed a non-regurgitant control condition and moderate regurgitation in both disease conditions. These measurements are summarized in Table 1.

MVP Condition

Composition—Sulfated GAG concentration was greater in MVP valve segments compared to controls (+37% anterior clear, +39% anterior rough, +72% posterior). MVP tissues also had greater hydration (+29% anterior clear, +33% anterior rough, +68% posterior). Immunohistochemistry showed a 188% greater level of collagen III expression in MVP posterior leaflets compared to controls, but no significant difference in anterior clear zone or anterior rough zone. MVP valve tissues were also significantly thicker than controls (+38% anterior clear, +49% anterior rough, +21% posterior circumferential, +43% anterior radial, +8% posterior radial). These results are summarized in Figure 5. Collagen content (Sircol Assay), MMP-1, Decorin, LOX, mature collagen (Herovici), and highly aligned collagen (picrosirius red) were analyzed and found to not be statistically significant.

Material Properties—MVP valve leaflets had a lower elastic modulus (−39% anterior clear, −59% anterior rough, −10% posterior circumferential, −14% anterior radial, −3% posterior radial) and lower ultimate stress (−50% anterior clear, −53% anterior rough, +2% posterior circumferential, −28% anterior radial, −39% posterior radial) than controls. In addition, the circumferentially oriented MVP leaflet segments had a significantly larger stress relaxation fast time constant (+6% anterior clear, +11% anterior rough, +6% posterior circumferential) compared to controls. This finding corresponds to greater viscosity over control tissues. Results are summarized in Figure 6.

FMR Condition

Composition—Compared to controls, FMR valve tissues had greater content of MMP-1, an interstitial collagenase involved in collagen degradation in remodeling tissues (+64% anterior clear, +73% anterior rough, +608% posterior). FMR valves also had greater expression of decorin, a small leucine-rich proteoglycan involved in collagen fibrillogenesis (+164% anterior clear, +64% anterior rough, +18% posterior), and LOX, an enzyme

responsible for collagen crosslinking (−15% anterior clear, +62% anterior rough, +193% posterior). Mature collagen content was also larger in FMR leaflets as captured by the percentage of red hue in the Herovici stain (+81% anterior clear, +57% anterior rough, +48% posterior). In addition, the amount of highly aligned collagen in FMR leaflets was lower than controls as measured by red birefringence of picrosirius red staining (−27% anterior clear, −36% anterior rough, −8% posterior). The Sircol analysis did not show a significant difference in overall collagen content between FMR and control valve tissues ($p = 0.50$). Results are shown in Figure 7. Collagen III, GAG concentration (Blyscan Assay), and hydration were analyzed and found not to be statistically significant.

Material Properties—FMR valve leaflets have a higher elastic modulus (+57% anterior clear, +48% anterior rough, +69% posterior circumferential, +17% anterior radial, +50% posterior radial) than control valves. Ultimate strain was lower in both radial FMR leaflet segments (−29% anterior radial, −46% posterior radial) and FMR chordae (−15% anterior basal, −9% posterior basal, −1% anterior marginal, −45% posterior marginal) when compared to control tissues. Extensibility was higher in circumferential FMR leaflets (+4% anterior clear, +13% anterior rough, +35% posterior), but lower in radial FMR leaflets (−48% anterior radial, −28% posterior radial) and chordae (−26% anterior basal, −17% posterior basal, +8% anterior marginal, −30% posterior marginal). Radial FMR leaflet segments also had a lower hysteresis percentage compared to controls (−35% anterior radial, −46% posterior radial), a sign of greater elasticity and lower viscosity in FMR tissues. Results are shown in Figure 8.

Discussion

Precise control of valve geometry allows for creation of clinically relevant disease hemodynamics

Using RUFLS, we have created the first sterile *in vitro* replication of mitral regurgitation. We previously established that dynamic culture of mitral valves in our organ culture system was significantly improved over static culture as comparable to fresh tissue.[18] This previous study showed that valves cultured within RUFLS maintained cell viability and proliferation. In addition, the system maintained sterility throughout the culture period and the pH of media was maintained.[17,18] However, that earlier work was limited in its ability to control annular and papillary muscle geometry. Previous systems in other labs have implemented precisely controlled geometry to recreate and investigate aspects of mitral valve disease in *in vitro* flow loops, but these studies were limited to non-sterile healthy valves without a long-term culture period.[6,25,41] In the work presented here, we aimed to replicate these advancements to better control papillary muscle positioning as well as annular diameter and shape, which allows for the first creation of mitral valve disease hemodynamics in a sterile *in vitro* system. By measuring and replicating the geometry of healthy valves in RUFLS, we are able to create a valve that is non-regurgitant throughout the one-week culture period. In addition, we confirmed that these improvements to RUFLS did not affect the previously established cell viability and proliferation of cultured tissues. Taking advantage of these improvements, we can recreate MVP and FMR-like valve geometries with moderate regurgitation and characteristic regurgitant color Doppler jet profiles *in vitro* by

manipulating the geometry of the valve from its neutral positioning. In addition, our measurements of regurgitation hemodynamics, assessed via echocardiography in our imaging flow loop, confirm the moderate regurgitation found in our sterile system flow meter measurements. We are therefore able to culture healthy valves in hemodynamic conditions that mimic clinical disease, investigating how the valve responds in a causal and controlled fashion. As a result, we can conclude that differences in tissues cultured in control versus disease conditions are due to the hemodynamic alterations mimicking the disease. This is an advantage of *in vitro* organ culture over clinical studies of diseased tissues, which cannot differentiate the impact of hemodynamic environment on tissue remodeling from underlying tissue pathology independent of environment.

MVP conditioned valve tissues undergo myxomatous remodeling

After one-week culture in the slack conditions resembling MVP, valve tissues showed characteristics of myxomatous remodeling. In the clinical presentation of mitral regurgitation, the most compelling evidence for myxomatous remodeling includes an elevation in GAG content,[21,22] higher amounts of type III collagen,[10] and a reduction in elastic modulus and ultimate stress compared to healthy valves.[3,4,22,23] Our MVP-conditioned valves have a similar set of differences from controls, with more reticular, type III collagen in the posterior leaflet, greater hydration, and elevated GAG content. The lack of significant findings amongst the collagen remodeling and synthesis enzymes investigated suggests that the low-tension environment of MVP results in a myxomatous phenotype through increased GAG and reticular collagen accumulation and not through extensive turnover of the existing collagen architecture. However, this does not preclude collagen enzyme involvement later in the remodeling process. The combination of these extracellular matrix changes results in altered material behavior in our valves including a reduction in elastic modulus and ultimate stress. In addition, a higher stress relaxation fast time constant in leaflets corresponds to more viscous behavior of MVP-conditioned valves compared to controls, consistent with greater GAG content.

Our ability to condition healthy valves to replicate these findings using hemodynamic manipulations alone helps to clarify the possible mechanisms of MVP pathology in a way that was previously impossible to obtain. Our findings support the hypothesis that the valvular interstitial cells of the mitral valve respond to the low-tension tissue conditions of MVP hemodynamics in a myxomatous manner, decreasing the tissue tensile strength in accordance with the hemodynamic demands placed on the tissue.

FMR condition valve tissues undergo fibrotic remodeling

After one-week culture in the high-tension environment of the FMR condition, valve tissues showed characteristics of fibrotic remodeling. Clinically, FMR tissues have been reported as having greater collagen content,[20] resulting in mechanically stiffer tissues compared to healthy controls.[19] Animal studies simulating FMR using tachycardia,[47] tethering,[12] and ischemia[42] also showed increases in collagen turnover, deposition, and procollagen I, respectively, consistent with fibrotic remodeling. While we did not find an elevation in collagen content, we did observe greater expression of factors involved with collagen fibrillar assembly (decorin), crosslinking (LOX), and degradation (MMP-1), as well as

increases in collagen maturity (Herovici staining). Taken together, these results suggest that FMR conditioned tissues are undergoing fibrotic remodeling.

The reorganization of collagen architecture within the valve plays an important role during fibrotic remodeling. The combination of smaller amounts of highly aligned collagen as measured by picrosirius red staining and increased presence of LOX, a collagen crosslinking enzyme, provides support for reorganization. This interpretation is also supported by the observed changes in material properties; FMR-conditioned tissues were stiffer, more brittle, less extensible, and less viscous than controls in the radial direction. These findings are consistent with the material property differences reported for human FMR leaflets, which were predominantly observed in radial specimens, oriented perpendicularly to the main collagen orientation in the mitral valve.[32] Collagen reorganization can also explain the larger extensibility in the circumferential direction, as a decrease in collagen alignment would necessitate more strain in order to incorporate and uncrimp the less aligned collagen components of the extracellular matrix.

These material properties also support the hypothesis that fibrotic-type remodeling is in response to the higher tension placed on valves by the hemodynamic conditions and tethering of FMR. Additionally, a majority of the observed mechanical alterations occurred in the radial direction, which experiences higher tension under tethering conditions. Also, larger elevations in MMP-1, LOX, and elastic modulus, as well as larger reductions in ultimate strain and hysteresis percentage, occurred in the posterior leaflet. As the posterior leaflet is under the least tension during healthy valve motion, finding that it reacts most strongly to high-tension FMR tethering demonstrates the effect of elevated tension on valve remodeling. This provides support for the hypothesis that mitral valve interstitial cells are responding to FMR hemodynamics by remodeling the extracellular matrix in a manner that increases stiffness and brittleness and decreases extensibility and viscosity of the valve. It also supports the previous findings that the mitral valve is not a passive actor in functional disease, and is physiologically altered as a result of the clinical setting seen in FMR.[20]

Implications of disease hemodynamics for remodeling

Both MVP and FMR are multifactorial disease processes. MVP has a wide variety of molecular and genetic mechanisms that may impact disease processes,[14] while FMR can result from a variety of causes of left ventricular regional or global dysfunction.[44] The final common pathway of both, however, is a regurgitant valve whose hemodynamic environment places aberrant mechanical forces on valve tissues throughout the cardiac cycle. By demonstrating that previously healthy valves placed in MVP and FMR hemodynamic conditions undergo myxomatous remodeling and fibrotic remodeling respectively, we have established a role for altered mechanics in the progression of mitral regurgitation.

These findings give insight to the development of mitral disease and how mitral tissues respond to alterations in hemodynamic and geometric conditions. While previous clinical studies have characterized these tissues in end-stage disease,[10,19] and animal studies have looked at the impact that imposed disease models in a physiological system have on the mitral valve,[12,47] our system allows for the investigation of the impact of isolated hemodynamic changes on valve tissues. By conditioning valves in our system and

comparing to controls cultured under identical pressure and heart rate conditions, we are able to establish a direct, causal relationship between altered hemodynamics created by our disease condition geometries and alterations that occur in tissues as a result. The dramatic differences observed show the profound impact that disease hemodynamics can impart upon valve remodeling, and the short, one-week culture time demonstrates that these changes happen quickly. Collectively, these findings suggest that the acute, large magnitude geometric changes imposed on valves in our system create an accelerated disease model of mitral regurgitation. Although mitral valve disease is typically a slowly developing chronic condition, the results of this work establish that the mitral valve is highly sensitive to changing mechanics. This mechanosensitivity could have implications for more acute forms of mitral regurgitation, such as ischemic mitral regurgitation. Ischemic mitral regurgitation occurs as a result of left ventricular dysfunction due to a myocardial infarction and is a form of acute functional mitral regurgitation.[5] In addition, there is much debate about the best clinical practice regarding the treatment of ischemic mitral regurgitation, especially in moderate and severe disease.[9,50] While clinical samples of mitral valve tissues from these patients have yet to be studied in the early stages of the disease, the left atria and left ventricle remodel rapidly in the weeks following infarct, suggesting a global cardiovascular remodeling event.[5] The results of our study suggest that such a hemodynamic alteration could also cause rapid remodeling of the mitral valve tissues.

Additionally, the increases in regurgitation observed in both disease models throughout the culture period provide evidence that valve remodeling worsens disease progression. In other words, the valves are not responding to the amount of regurgitant flow, but rather to the mechanical load placed on the valves as a result of valve geometry and hemodynamics. This load then leads to tissue remodeling that worsens the regurgitation. These findings also provide support for the hypothesis that the mitral valve is an active participant in the disease process of both organic (MVP) and functional (FMR) valve disease. Additionally, this interaction challenges the notion that valve disease is distinctly an organic or functional phenomenon. While it is still useful to classify mitral valve disease in terms of whether the inciting pathologic incident was intrinsic to the valve (organic) or due to disturbances in valve geometry (functional), our findings suggest that the disease progression is a dynamic interaction between the compositional properties of the valves and the resulting forces. Intervention, if it restores native valve geometry as a part of repair, could respond in a similarly rapid fashion. Recent findings suggest that when repairs of ischemic mitral regurgitation do fail, the increasing post-repair regurgitation is correlated with the presence of leaflet tethering, in isolation of regurgitation volume after surgery.[31] This finding supports our finding that the mitral valve remodels -- in a way that results in increased regurgitation -- when placed under pathologic mechanics such as the tethering of leaflets. Several experimental devices have aimed to address the concern that eliminating regurgitation alone is not adequate for long-term repair if the valve is still experiencing altered mechanics. Devices such as the Coapsys[16] and Mitral Touch[48] aim to reposition the papillary muscles of the mitral valve in order to create a more lasting treatment for FMR. While further study is needed to explore how rapidly and in what context myxomatous and fibrotic remodeling can be reversed, the findings of dynamic adaptation of the valve in response to changing

mechanical environment does lend support to the idea that removing the pathologic mechanical environment could quickly impact valve remodeling.

The re-creation of mitral regurgitation *in vitro* is a useful method to evaluate the effect of altered tension on mitral valve leaflet remodeling, so long as the results are considered within the appropriate context. For example, RUFLS cannot replicate the systemic physiologic response to the disease geometries that were imposed on healthy mitral valves to create our models. This limitation includes the lack of systemic cardiovascular response to reduce the imposed regurgitation and alterations in blood pressure that would result. Physiological responses would also include cellular or healing responses that would initiate from sources outside the valve in response to the disease state. However, although this system lacks physiologic response that would be observed clinically or in an animal model, it does allow for the control of the hemodynamic environment that would not be possible in a physiologically responsive system. This control allows for direct conclusions on how disease hemodynamics affects living valve tissues. A limitation of the RUFLS system is the sub-physiological flow of 3 L/min, which was the result of constraints placed on different RUFLS components due to the requirements of sterile culture. This lower flow rate reduces shear stress experienced by valve leaflets within our system and could affect the response of valves as a result. Another limitation of this study is the use of a flat annulus during culture. The native annulus is saddle shaped, and this shape has been shown to have an impact on valve function throughout the cardiac cycle.[28,40] Additionally, while porcine valves provide the closest animal model of human mitral valves, slight anatomical differences could affect the translation of these findings to human disease.

By exploring the impact of mechanical forces on remodeling in two distinct disease conditions, our *in vitro* systems provide an experimental paradigm for the further investigation of MVP and FMR remodeling and ways to reverse it. This work establishes the dynamic interaction between composition, mechanical properties of valve tissues, and the mechanical environment of regurgitation, and how the interplay between these three factors leads to the progression of mitral regurgitation. The highly controlled and modular nature of valve models and our ability to perform functional imaging of the valve constructs will allow us to explore the independent effects of additional geometric, hemodynamic, or pharmacological alterations to control, MVP, and FMR valves in a timely fashion without the confounding impacts of systemic physiological responses. While clinical and animal studies remain invaluable resources for disease investigation, the establishment of *in vitro* disease conditioning provides a highly controlled mechanism for investigating disease progression and potentially reversal.

Supplementary Material

Refer to Web version on PubMed Central for supplementary material.

Acknowledgments

The authors would like to acknowledge Dr. Larry Fisher, NIH, for his gift of decorin antibody used in the course of this research. This work was supported by the National Institutes of Health [T32HL007676] and the American Heart Association [13PRE14110003 to P.C.].

Abbreviations

FMR	functional mitral regurgitation
GAG	glycosaminoglycan
LOX	lysyl oxidase
MMP-1	matrix metalloproteinase-1
MVP	mitral valve prolapse
RUFLS	Rice University flow loop system

References

1. De Agustín JA, Marcos-Alberca P, Fernandez-Golfin C, Gonçalves A, Feltes G, Nuñez-Gil IJ, Almeria C, Rodrigo JL, Perez de Isla L, Macaya C, Zamorano J. Direct measurement of proximal isovelocity surface area by single-beat three-dimensional color Doppler echocardiography in mitral regurgitation: a validation study. J Am Soc Echocardiogr. 2012; 25:815–23. [PubMed: 22739217]
2. Balaoing LR, Post AD, Liu H, Minn KT, Grande-Allen KJ. Age-related changes in aortic valve hemostatic protein regulation. Arterioscler Thromb Vasc Biol. 2014; 34:72–80. [PubMed: 24177329]
3. Barber JE, Kasper FK, Ratliff NB, Cosgrove DM, Griffin BP, Vesely I. Mechanical properties of myxomatous mitral valves. J Thorac Cardiovasc Surg. 2001; 122:955–962. [PubMed: 11689801]
4. Barber JE, Ratliff NB, Cosgrove DM, Griffin BP, Vesely I. Myxomatous mitral valve chordae. I: Mechanical properties. J Heart Valve Dis. 2001; 10:320–4. [PubMed: 11380094]
5. Benjamin MM, Smith RL, Grayburn Pa. Ischemic and Functional Mitral Regurgitation in Heart Failure: Natural History and Treatment. Curr Cardiol Rep. 2014; 16:517. [PubMed: 24957516]
6. Bhattacharya S, He Z. Annulus tension of the prolapsed mitral valve corrected by edge-to-edge repair. J Biomech. 2012; 45:562–8. [PubMed: 22153221]
7. Boltwood CM, Tei C, Wong M, Shah PM. Quantitative echocardiography of the mitral complex in dilated cardiomyopathy: the mechanism of functional mitral regurgitation. Circulation. 1983; 68:498–508. [PubMed: 6872163]
8. Carew EO, Vesely I. A new method of estimating gauge length for porcine aortic valve test specimens. J Biomech. 2003; 36:1039–42. [PubMed: 12757813]
9. Chan KMJ, Punjabi PP, Flather M, Wage R, Symmonds K, Roussin I, Rahman-Haley S, Pennell DJ, Kilner PJ, Dreyfus GD, Pepper JR. Coronary artery bypass surgery with or without mitral valve annuloplasty in moderate functional ischemic mitral regurgitation: Final results of the Randomized Ischemic Mitral Evaluation (RIME) trial. Circulation. 2012; 126:2502–2510. [PubMed: 23136163]
10. Cole WG, Chan D, Hickey AJ, Wilcken DE. Collagen composition of normal and myxomatous human mitral heart valves. Biochem J. 1984; 219:451–460. [PubMed: 6430269]
11. Croft LR, Jimenez JH, Gorman RC, Gorman JH, Yoganathan AP. Efficacy of the edge-to-edge repair in the setting of a dilated ventricle: an in vitro study. Ann Thorac Surg. 2007; 84:1578–84. [PubMed: 17954065]
12. Dal-Bianco JP, Aikawa E, Bischoff J, Guerrero JL, Handschumacher MD, Sullivan S, Johnson B, Titus JS, Iwamoto Y, Wylie-Sears J, Levine RA, Carpentier A. Active adaptation of the tethered mitral valve: insights into a compensatory mechanism for functional mitral regurgitation. Circulation. 2009; 120:334–42. [PubMed: 19597052]
13. Dayan D, Hiss Y, Hirshberg A, Bubis JJ, Wolman M. Are the polarization colors of Picrosirius red-stained collagen determined only by the diameter of the fibers ? Histochemistry. 1989; 93:27–9. [PubMed: 2482274]
14. Delling FN, Vasan RS. Epidemiology and pathophysiology of mitral valve prolapse: New insights into disease progression, genetics, and molecular basis. Circulation. 2014; 129:2158–2170. [PubMed: 24867995]

15. Fisher LW, Stubbs JT, Young MF. Antisera and cDNA probes to human and certain animal model bone matrix noncollagenous proteins. Acta Orthop Scand Suppl. 1995; 266:61–5. [PubMed: 8553864]
16. Fukamachi K, Popović ZB, Inoue M, Doi K, Schenk S, Ootaki Y, Kopcak MW, McCarthy PM. Changes in mitral annular and left ventricular dimensions and left ventricular pressure-volume relations after off-pump treatment of mitral regurgitation with the Coapsys device. Eur J Cardiothorac Surg. 2004; 25:352–7. [PubMed: 15019660]
17. Gheewala N, Grande-Allen KJ. Design and Mechanical Evaluation of a Physiological Mitral Valve Organ Culture System. Cardiovasc Eng Technol. 2010; 1:123–131.
18. Gheewala N, Schwarz KA, Grande-Allen KJ. Organ Culture of Porcine Mitral Valves as a Novel Experimental Paradigm. Cardiovasc Eng Technol. 2013; 4:139–150.
19. Grande-Allen KJ, Barber JE, Klatka KM, Houghtaling PL, Vesely I, Moravec CS, McCarthy PM. Mitral valve stiffening in end-stage heart failure: evidence of an organic contribution to functional mitral regurgitation. J Thorac Cardiovasc Surg. 2005; 130:783–90. [PubMed: 16153929]
20. Grande-Allen KJ, Borowski AG, Troughton RW, Houghtaling PL, Dipaola NR, Moravec CS, Vesely I, Griffin BP. Apparently normal mitral valves in patients with heart failure demonstrate biochemical and structural derangements: an extracellular matrix and echocardiographic study. J Am Coll Cardiol. 2005; 45:54–61. [PubMed: 15629373]
21. Grande-Allen KJ, Griffin BP, Calabro A, Ratliff NB, Cosgrove DM, Vesely I. Myxomatous mitral valve chordae. II: Selective elevation of glycosaminoglycan content. J Heart Valve Dis. 2001; 10:325–332. discussion 332–333. [PubMed: 11380095]
22. Grande-Allen KJ, Griffin BP, Ratliff NB, Cosgrove DM, Vesely I. Glycosaminoglycan profiles of myxomatous mitral leaflets and chordae parallel the severity of mechanical alterations. J Am Coll Cardiol. 2003; 42:271–277. [PubMed: 12875763]
23. Grande-Allen KJ, Liao J. The heterogeneous biomechanics and mechanobiology of the mitral valve: implications for tissue engineering. Curr Cardiol Rep. 2011; 13:113–20. [PubMed: 21221857]
24. Granier M, Jensen MO, Honge JL, Bel A, Menasché P, Nielsen SL, Carpentier A, Levine Ra, Hagège Aa. Consequences of mitral valve prolapse on chordal tension: ex vivo and in vivo studies in large animal models. J Thorac Cardiovasc Surg. 2011; 142:1585–7. [PubMed: 21955468]
25. He S, Fontaine AA, Schwammenthal E, Yoganathan AP, Levine RA. Integrated Mechanism for Functional Mitral Regurgitation. Circulation. 1997; 96:1826. [PubMed: 9323068]
26. Herovici C. A polychrome stain for differentiating precollagen from collagen. Stain Technol. 1963; 38:204. [PubMed: 13959845]
27. Jimenez JH, Ritchie J, He Z, Yoganathan AP. Mechanics of the mitral valve: in vitro studies. Conf Proc IEEE Eng Med Biol Soc. 2004; 5:3727–3729. [PubMed: 17271104]
28. Jimenez JH, Soerensen DD, He Z, He S, Yoganathan AP. Effects of a Saddle Shaped Annulus on Mitral Valve Function and Chordal Force Distribution: An In Vitro Study. Ann Biomed Eng. 2003; 31:1171–1181. [PubMed: 14649491]
29. Jimenez JH, Soerensen DD, He Z, Ritchie J, Yoganathan AP. Effects of papillary muscle position on chordal force distribution: an in-vitro study. J Heart Valve Dis. 2005; 14:295–302. [PubMed: 15974521]
30. Junqueira LC, Bignolas G, Brentani RR. Picrosirius staining plus polarization microscopy, a specific method for collagen detection in tissue sections. Histochem J. 1979; 11:447–55. [PubMed: 91593]
31. Kron IL, Hung J, Overbey JR, Bouchard D, Gelijns AC, Moskowitz AJ, Voisine P, O'Gara PT, Argenziano M, Michler RE, Gillinov M, Puskas JD, Gammie JS, Mack MJ, Smith PK, Sai-Sudhakar C, Gardner TJ, Ailawadi G, Zeng X, O'Sullivan K, Parides MK, Swayze R, Thourani V, Rose Ea, Perrault LP, Acker Ma. Predicting recurrent mitral regurgitation after mitral valve repair for severe ischemic mitral regurgitation. J Thorac Cardiovasc Surg. 2015; 149:752–761.e1. [PubMed: 25500293]
32. Kunzelman KS, Cochran RP. Stress/strain characteristics of porcine mitral valve tissue: parallel versus perpendicular collagen orientation. J Card Surg. 1992; 7:71–78. [PubMed: 1554980]

33. Lacerda CMR, Kisiday J, Johnson B, Orton EC. Local serotonin mediates cyclic strain-induced phenotype transformation, matrix degradation, and glycosaminoglycan synthesis in cultured sheep mitral valves. Am J Physiol Hear Circ Physiol. 2012; 302:H1983–90.
34. Lacerda CMR, Maclea HB, Kisiday JD, Orton EC. Static and cyclic tensile strain induce myxomatous effector proteins and serotonin in canine mitral valves. J Vet Cardiol. 2012; 14:223–30. [PubMed: 22364693]
35. Little SH, Igo SR, McCulloch M, Hartley CJ, Nosé Y, Zoghbi Wa. Three-dimensional ultrasound imaging model of mitral valve regurgitation: design and evaluation. Ultrasound Med Biol. 2008; 34:647–54. [PubMed: 18255217]
36. Little SH, Igo SR, Pirat B, McCulloch M, Hartley CJ, Nosé Y, Zoghbi WA. In vitro validation of real-time three-dimensional color Doppler echocardiography for direct measurement of proximal isovelocity surface area in mitral regurgitation. Am J Cardiol. 2007; 99:1440–1447. [PubMed: 17493476]
37. Nielsen SL, Nygaard H, Fontaine AA, Hasenkam JM, He S, Andersen NT, Yoganathan AP. Chordal force distribution determines systolic mitral leaflet configuration and severity of functional mitral regurgitation. J Am Coll Cardiol. 1999; 33:843–53. [PubMed: 10080490]
38. Nielsen SL, Nygaard H, Mandrup L, Fontaine Aa, Hasenkam JM, He S, Yoganathan AP. Mechanism of Incomplete Mitral Leaflet Coaptation—Interaction of Chordal Restraint and Changes in Mitral Leaflet Coaptation Geometry. J Biomech Eng. 2002; 124:596. [PubMed: 12405603]
39. Otsuji Y. Isolated Annular Dilation Does Not Usually Cause Important Functional Mitral Regurgitation. 2002; 39:0–5.
40. Padala M, Hutchison Ra, Croft LR, Jimenez JH, Gorman RC, Gorman JH, Sacks MS, Yoganathan AP. Saddle shape of the mitral annulus reduces systolic strains on the P2 segment of the posterior mitral leaflet. Ann Thorac Surg. 2009; 88:1499–504. [PubMed: 19853100]
41. Padala M, Powell SN, Croft LR, Thourani VH, Yoganathan AP, Adams DH. Mitral valve hemodynamics after repair of acute posterior leaflet prolapse: quadrangular resection versus triangular resection versus neochordoplasty. J Thorac Cardiovasc Surg. 2009; 138:309–15. [PubMed: 19619772]
42. Quick DW, Kunzelman KS, Kneebone JM, Cochran RP. Collagen synthesis is upregulated in mitral valves subjected to altered stress. ASAIO J. 1997; 43:181–6. [PubMed: 9152488]
43. Rich L, Whittaker P. Collagen and picrosirius red staining: a polarized light assessment of fibrillar hue and spatial distribution. Braz J Morphol Sci. 2005; 22:97–104.
44. Rossi A, Dini FL, Faggiano P, Agricola E, Cicoira M, Frattini S, Simioniuc A, Gullace M, Ghio S, Enriquez-Sarano M, Temporelli PL. Independent prognostic value of functional mitral regurgitation in patients with heart failure. A quantitative analysis of 1256 patients with ischaemic and non-ischaemic dilated cardiomyopathy. Heart. 2011; 97:1675–80. [PubMed: 21807656]
45. Stephens EH, Carroll JL, Grande-Allen KJ. The use of collagenase III for the isolation of porcine aortic valvular interstitial cells: rationale and optimization. J Heart Valve Dis. 2007; 16:175–83. [PubMed: 17484468]
46. Stephens EH, Grande-Allen KJ. Age-related changes in collagen synthesis and turnover in porcine heart valves. J Heart Valve Dis. 2007; 16:672–82. [PubMed: 18095519]
47. Stephens EH, Timek TA, Daughters GT, Kuo JJ, Patton AM, Baggett LS, Ingels NB, Miller DC, Grande-Allen KJ. Significant changes in mitral valve leaflet matrix composition and turnover with tachycardia-induced cardiomyopathy. Circulation. 2009; 120:S112–9. [PubMed: 19752355]
48. Takaseya T, Shiose A, Saraiva RM, Fumoto H, Arakawa Y, Juravic M, Lombardi P, Fukamachi K. Novel epicardial off-pump device for mitral regurgitation: acute evaluation. Eur J Cardiothorac Surg. 2010; 37:1291–6. [PubMed: 20137971]
49. Thavendiranathan P, Liu S, Datta S, Rajagopalan S, Ryan T, Igo SR, Jackson MS, Little SH, De Michelis N, Vannan Ma. Quantification of chronic functional mitral regurgitation by automated 3-dimensional peak and integrated proximal isovelocity surface area and stroke volume techniques using real-time 3-dimensional volume color doppler echocardiography: In vitro and clini. Circ Cardiovasc Imaging. 2013; 6:125–133. [PubMed: 23223636]

50. Zhang Y, Ma L, Zhao H. Efficacy of Mitral Valve Repair as an Adjunct Procedure to Coronary Artery Bypass Grafting in Moderate Ischemic Mitral Regurgitation: A Meta-Analysis of Randomized Trials. J Card Surg. 2015:n/a–n/a.10.1111/jocs.12585

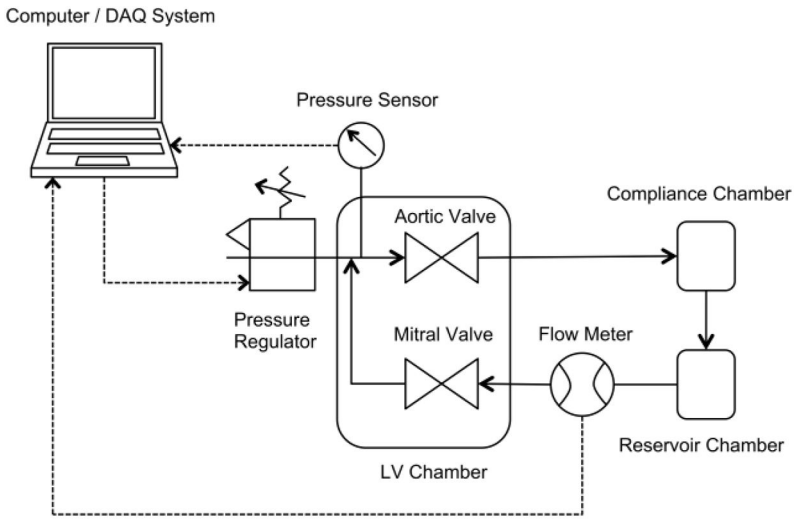

Figure 1.

Schematic of Rice University Flow Loop System (RUFLS). Solid arrows show the flow of media through the bioreactor system. Dashed arrows show the flow of information to and from RUFLS and the computer DAQ system. LV = left ventricle. DAQ = data acquisition system.

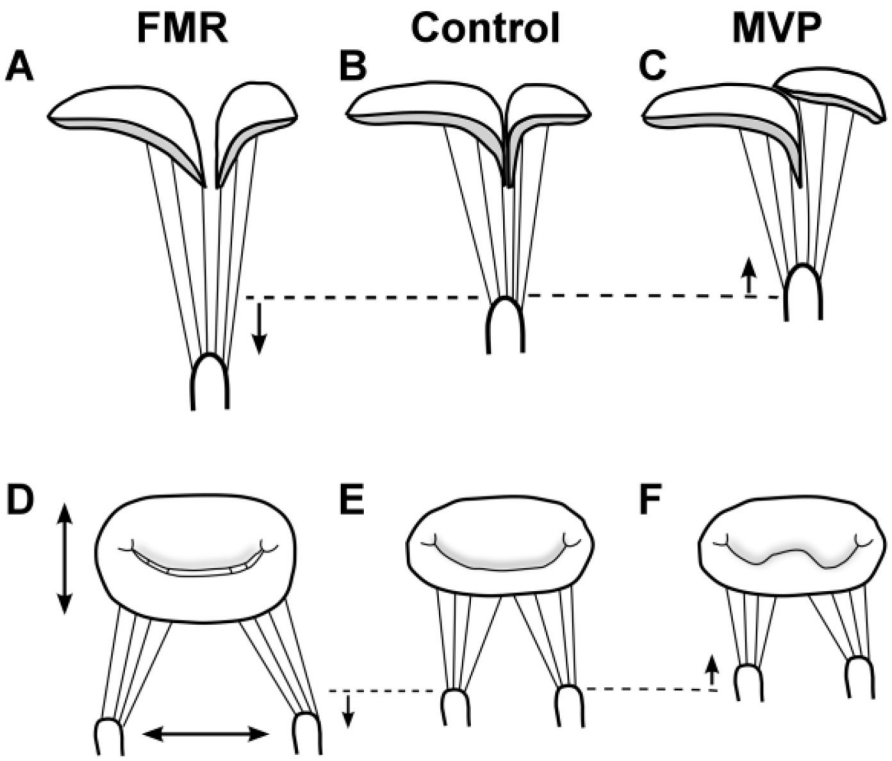

Figure 2.

MVP & FMR Condition Creation. FMR condition created by (A) apical and (D) lateral displacement of papillary muscles from the neutral position (dashed line), as well as (D) 65% greater annular area compared to (E) control annulus. (C, F) MVP model created by basal displacement of papillary muscles from neutral position (dashed line). (B, E) Control model created by placing valve in neutral position. FMR = functional mitral regurgitation; MVP = mitral valve prolapse.

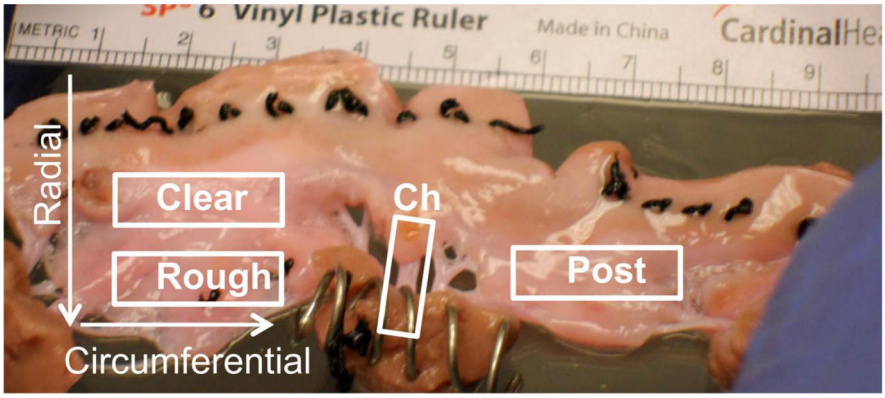

Figure 3.

Valve Sections. Tissues were mechanically tested in radial and circumferential directions and the anterior leaflet was divided into clear and rough zones corresponding to the absence or presence of chordae tendineae.

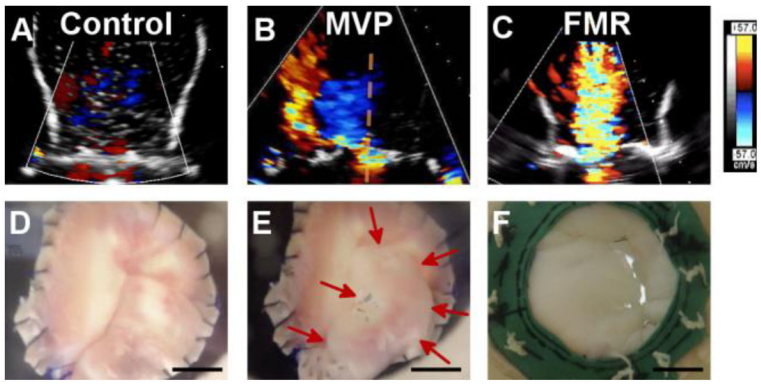

Figure 4.

Analysis of Valve Models. Using the Imaging Flow Loop, (A) control valves showed no regurgitant jet. (B) MVP valves showed characteristic eccentric regurgitant jet (red, left-oriented back flow). (C) FMR valves showed characteristic central jet. Photos (bottom row) are screen shots taken during end of systole from imaging flow loop videos. (D) Controls with proper coaptation of leaflets. (E) MVP posterior leaflet prolapsing (red arrows emphasize prolapsing leaflet). (F) FMR leaflets tethering resulting in incomplete coaptation. n = 2. Scale bar = 1 cm. FMR = functional mitral regurgitation; MVP = mitral valve prolapse.

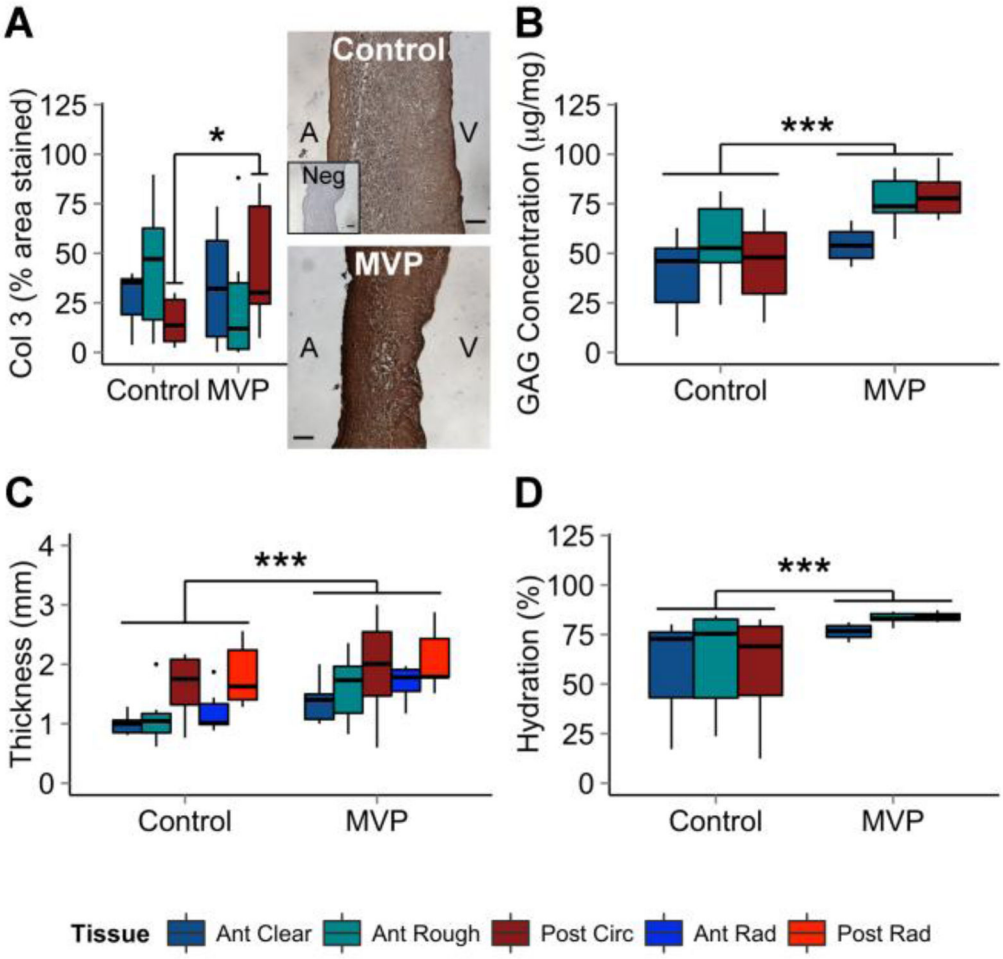

Figure 5.

Myxomatous Characteristics Elevated in MVP. MVP leaflets have higher concentrations of (A) Col3 as calculated by the percent area stained using immunohistochemistry. In addition, (B) MVP leaflets have higher concentrations of GAGs, (C) are thicker, and (D) have greater hydration compared to controls. Representative pictures of DAB-based immunohistochemistry staining of controls (top picture), negative controls (no primary antibody; insert, top picture), and MVP valves (bottom picture) are shown. n = 6 to 8. Scale bar = 100 µm. ANOVA with post hoc Tukey's HSD test used for significance. * = $p < 0.05$; ** = $p < 0.01$; *** = $p < 0.001$. Col3 = collagen III; GAG = glycosaminoglycan; MVP = mitral valve prolapse; Neg = negative control.

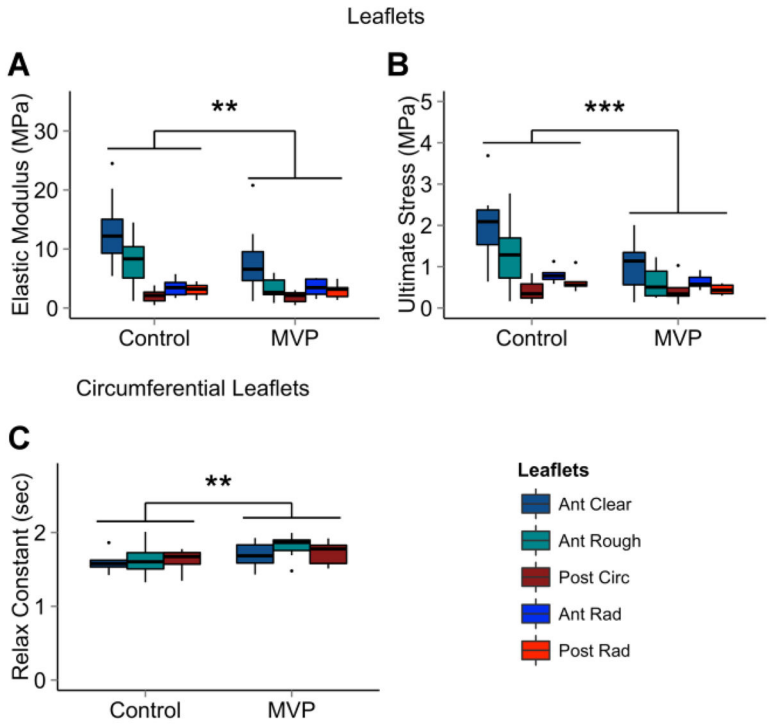

Figure 6.

Mechanical Analysis of MVP Valves. MVP leaflets have (A) lower elastic modulus and (B) lower ultimate stress overall. In addition, MVP leaflets have (C) a larger stress relaxation fast time constant than controls in the circumferential direction. n = 6 to 8 leaflets, 14 to 16 chordae. ANOVA with post hoc Tukey's HSD test used for significance. * = $p < 0.05$; ** = $p < 0.01$; *** = $p < 0.001$.

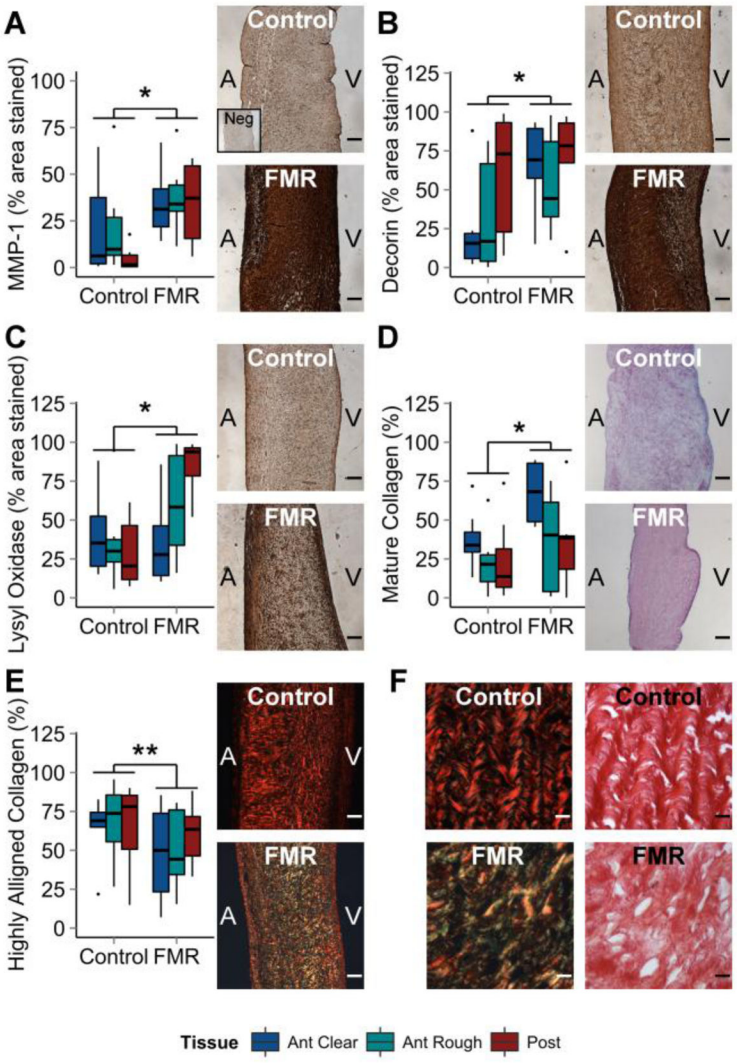

Figure 7.

Fibrotic Remodeling Characteristics Elevated in FMR. FMR leaflets have higher concentrations of (A) MMP-1, (B) decorin, and (C) lysyl oxidase as calculated by the percent area stained using immunohistochemistry (graphs). In addition, FMR leaflets have (D) more mature collagen as measured by red hue in Herovici staining but (E) less aligned collagen as measured by red birefringence in picrosirius red staining. (F) Representative, higher resolution images of picrosirius red staining in polarized and white light are shown, along with representative pictures of (A–C) DAB-based immunohistochemistry and (D) Herovici staining of controls and FMR valves. n = 6 to 8. Scale bar = 100 μm (A–E) or 800 μm (F). ANOVA with post hoc Tukey's HSD test used for significance. * = $p < 0.05$; ** = $p < 0.01$; *** = $p < 0.001$. FMR = functional mitral regurgitation; MMP-1 = matrix metalloproteinase 1; Neg = negative control.

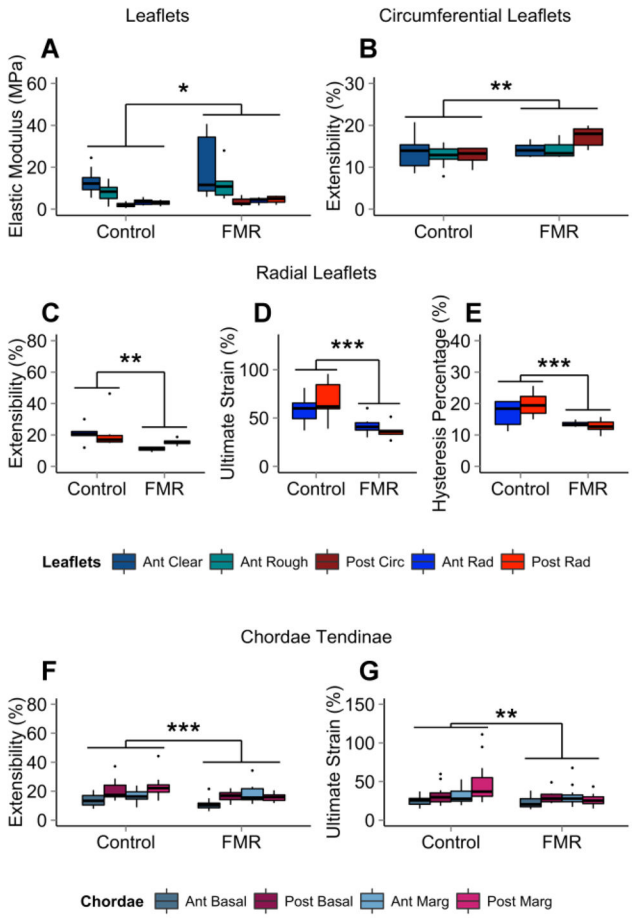

Figure 8.

Mechanical Analysis of FMR Valves. FMR leaflets had (A) higher elastic modulus than controls. In the circumferential direction, FMR valves had (B) higher extensibility. In the radial direction, FMR leaflets had (C) lower extensibility, (D) lower ultimate strain, and (E) lower hysteresis percentage than controls. FMR chordae had (F) less extensibility and (G) lower ultimate strain than controls. n = 6 to 8 leaflets, 14 to 16 chordae. ANOVA with post hoc Tukey's HSD test used for significance. * = $p < 0.05$; ** = $p < 0.01$; *** = $p < 0.001$. FMR = functional mitral regurgitation.

Table 1

Hemodynamic Validation of Regurgitant Conditions Using Echocardiography.

Condition	Control	MVP	FMR
Flowmeter regurgitant flow volume (ml)	-	40	43
Leaflet coaptation length (mm)	16	9	6
Vena contracta			
Long axis (mm)	-	5	4
Short axis (mm)	-	4	11
Area (cm^2)	-	0.34	0.29
PISA effective regurgitant orifice area (cm^2)	-	0.3	0.2*
PISA derived regurgitant volume (ml)	-	27	37

*PISA method well recognized to underestimate effective regurgitant orifice area for FMR[1,49]